Environment
www.csiro.au

Initial exploration of the 2023 stock assessment models

R. Hillary, A. Preece, C. Davies, L. Tremblay-Boyer

CSIRO Environment
Battery Point, Hobart 7000, Tasmania, Australia.

Contents

1 Background

This document details an initial exploration of the data inputs, reference grid configuration, data fits and population dynamic summaries in preparation for the upcoming 2023 stock assessment.

2 Data inputs

The data inputs are the same as the previous assessment [1]:

- Catch biomass and age (Indonesian, surface) or size (longline fleets) frequency by fishery
- Longline CPUE (fleet LL_1) relative abundance index (1969–2022)
- Aerial survey juvenile relative biomass index (1993–2017)
- Mark-recapture data (1990–1994 & 1–3 release years & ages)
- Gene tagging age 2 absolute abundance estimates (2016–2021)
- CKMR Parent-Offspring Pairs (POPs) (2002–2018)
- CKMR Half-Sibling Pairs (HSPs) (2003–2017)

3 Reference grid configuration

Each stock assessment explores in detail what the appropriate grid configuration should. The grid used in the previous stock assessment [1] is used as the initial grid explored for the next scheduled assessment (Table 3.1). The only change is that we now have a single longline CPUE index [2], thereby reducing the number of grid elements to 216 fro 432. As in previous assessments and OM reconditioning 2,000 grids are drawn, according to the resampling strategy detailed in Table 3.1, from the now 216 unique grid elements. It is from these 2,000 grids that we assess the fits to the data, and summarise the key population dynamic and fishery variables of interest. Figure 3.1 details the summary level plot for the initial grid configuration detailed in Table 3.1.

Parameter	Values	Prior	Resampling	CumulN
Steepness	$\{0.55, 0.63, 0.72, 0.8\}$	Uniform	Prior	4
M_0	$\{0.4, 0.45, 0.5\}$	Uniform	Objf	12
M_{10}	$\{0.065, 0.085, 0.1025\}$	Uniform	Objf	36
ω	$\{1\}$	Uniform	Prior	36
CPUE index	$\{1\}$	Uniform	Prior	36
CPUE ages	$\{4, 18\}$ & $\{8, 12\}$	$\{0.67, 0.33\}$	Prior	72
ψ	$\{1.5, 1.75, 2\}$	$\{0.25, 0.5, 0.25\}$	Prior	216

Table 3.1: *Initial grid configuration for exploration of 2023 stock assessment.*

4 Fits to data sources

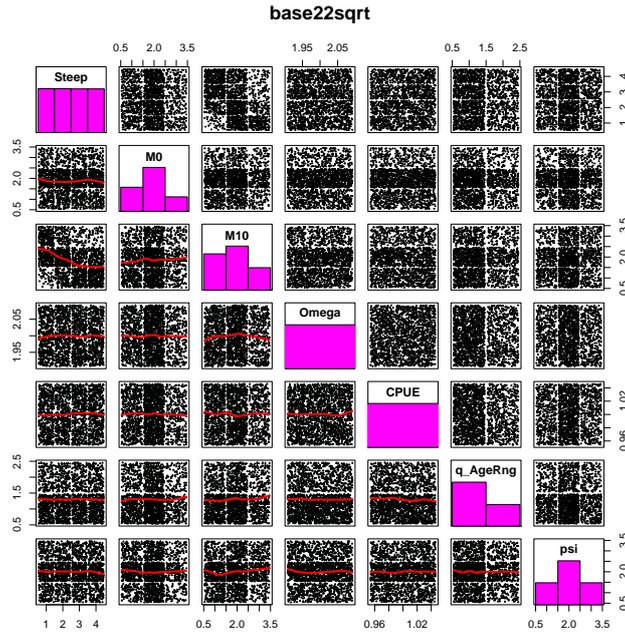Fits to the input data sources are summarised by general grouping.

Figure 3.1: *Level plot for the initial grid configuration for the 2023 assessment (base22).*

4.1 Fishery age & size frequency

Fit summaries for these data are detailed for the best fitting grid element. Figure 4.1 details the fitting summary for the Indonesian and surface fisheries.
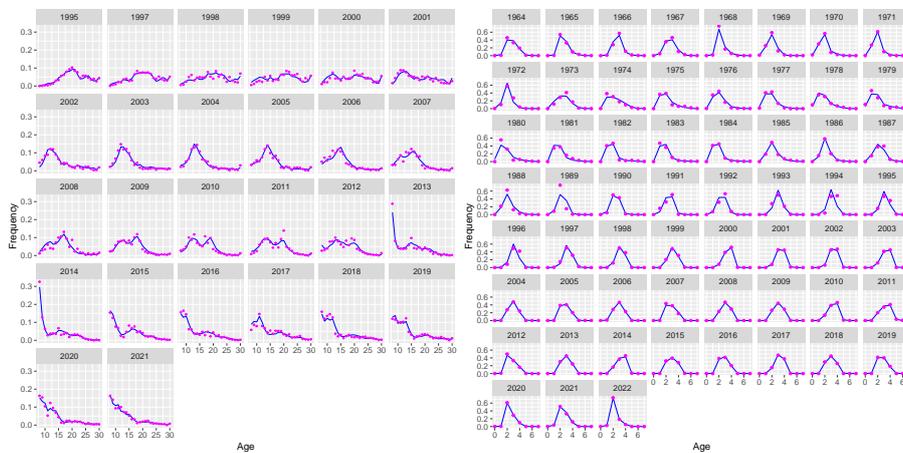

Figure 4.1: *Fits to Indonesian (left) and surface (right) age frequency data for the best fitting grid element. Magenta dots are the observations and blue lines are the predictions.*

The main longline fishery is LL_1 and Figure 4.2 summarises the fits to these data. Figure 4.3 summarises the fits to the size data for the other longline fisheries.

4.2 Abundance indices

For the abundance indices we have taken a predictive distribution approach to summarising the fits to the data. This is an approximation to what is known as posterior predictive analysis [4] - observations are simulated from their posterior distribution jointly accounting for both observation
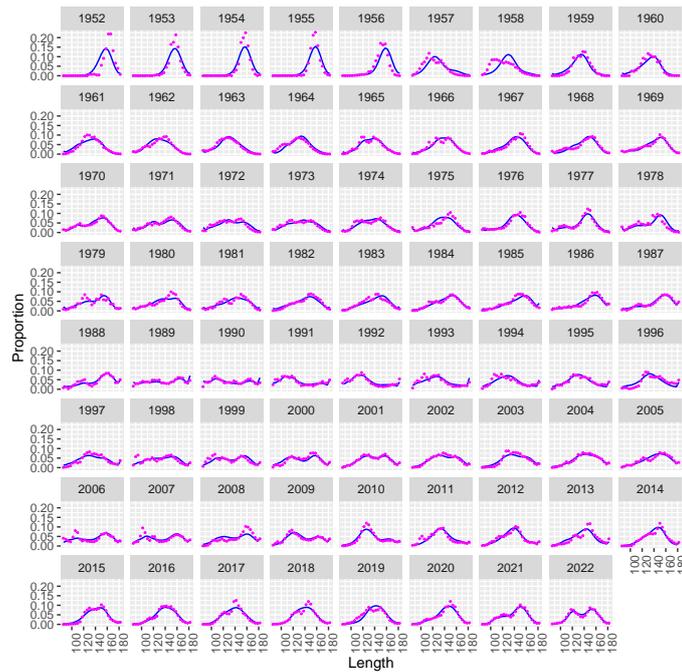
Figure 4.2: *Fits to LL_1 size frequency data for the best fitting grid element. Magenta dots are the observations and blue lines are the predictions.*

error and parametric uncertainty. The approximation used (given the grid doesn't represent a true posterior distribution in the Bayesian sense) simulates the observations from their likelihood and across all the grid elements. This jointly accounts for both observation error and grid parametric uncertainty, so we can assess how well the set of OMs is explaining the data. As well as the predictive distribution we also generate an analogue of the posterior predictive p-value [5]: the probability with which some suitable (preferably sufficient) statistic summarising the degree to which the variability in the observations exceeds that of the predictions. An ideal value of this p-value would be 0.5, with values outside of the 0.05–0.95 range deemed worthy of further exploration [5]. Figure 4.4 details the predictive summaries for the LL CPUE and aerial survey abundance indices for the initial reference grid. In terms of predictive p-values for the CPUE the value was 0.1 and for the aerial survey 0.87 - this is a result of the long-term and deliberate choice to increase the observation error of the CPUE and decrease the process error of the aerial survey [3].

4.3   Conventional mark-recapture

For the conventional tagging data of the 1990s we use the best fitting grid element and focus on: (i) recaptures aggregated across tagger groups; and (ii) recaptures aggregated across tagger groups and release ages. Figure 4.4 details the appropriately aggregated tagging fitting summaries. The tagging over-dispersion factor was previously set at 1.82 (variance inflation relative to the underlying default multinomial distribution) [3]. Inspection of the standardised residuals in the tagging predictions - does their variance differ from 1 - shows that this over-dispersion value is still the most appropriate value for these data.
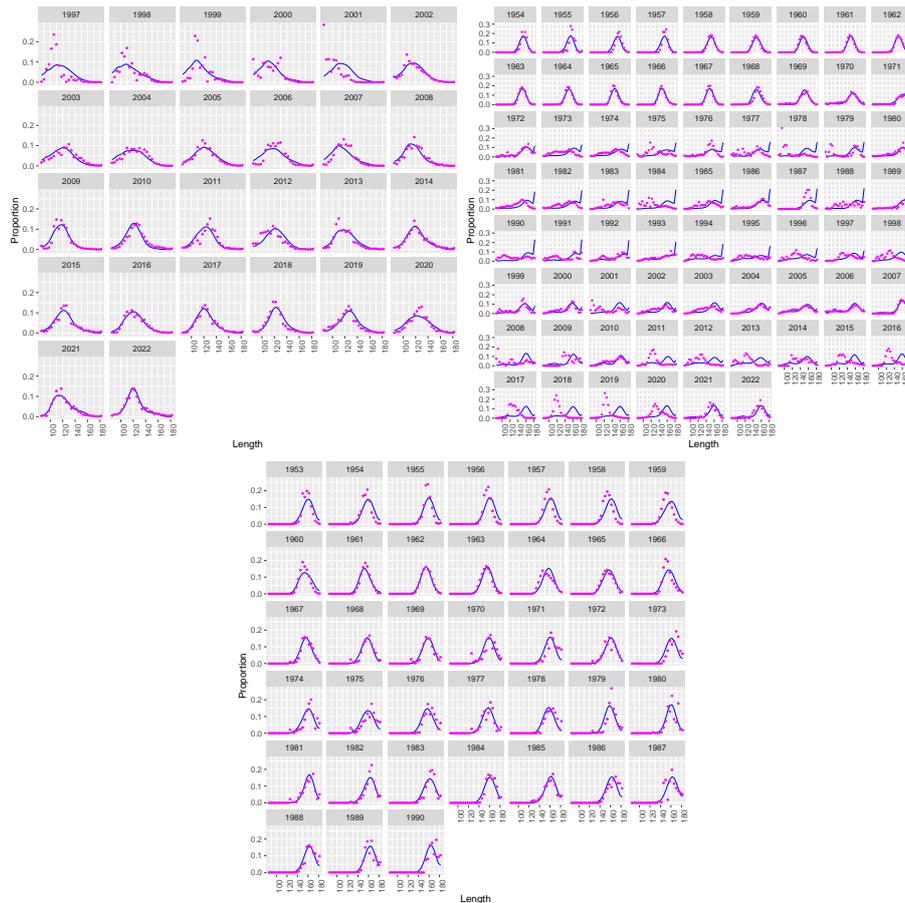
Figure 4.3: *Fits to LL_2 (left), LL_3 (right), and LL_4 (bottom) size frequency data for the best fitting grid element. Magenta dots are the observations and blue lines are the predictions.*

4.4 Gene tagging

The use of the gene tagging is as done previously: the probability of recapturing an age 3 fish given its release at age 2 the previous year is inversely proportional to the absolute abundance of the age 2 fish in the population. The current default distribution of the number of matches is binomial. Figure 4.6 details the predictive summary of the gene tagging matches given the observations.

4.5 Close-Kin Mark-Recapture

The CKMR data sets are the Parent-Offspring (POP) and Half-Sibling (HSP) pairs - two data sets that are treated as conditionally independent given the population dynamic variables that define their probabilities. In both cases, previous work has verified that a binomial distribution is an appropriate likelihood [3]. Previous assessments have dealt with the sparse nature of these data - in particular the POPs - by aggregating the summaries to more meaningful levels. For the POPs this includes:

1. Juvenile birth cohort - aggregating across adult capture year and age

2. Adult capture age - aggregating across juvenile cohort and adult capture year

3. Adult capture year - aggregating across juvenile cohort and adult capture age

The intention is that these capture: (i) overall adult abundance; (ii) age structure of the POPs; (iii)
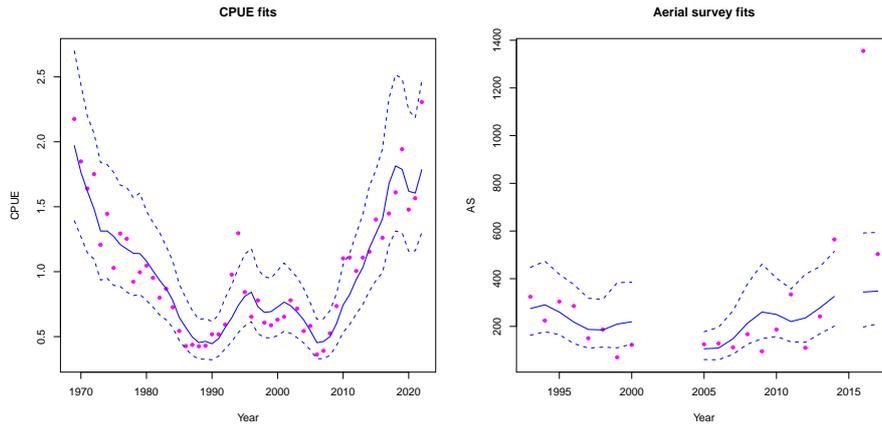
Figure 4.4: *Predictive summary for LL CPUE (left) and the aerial survey (right) abundance indices, respectively. Magenta dots are the observations and blue full and dotted lines are the predictive median and 95% interval, respectively.*
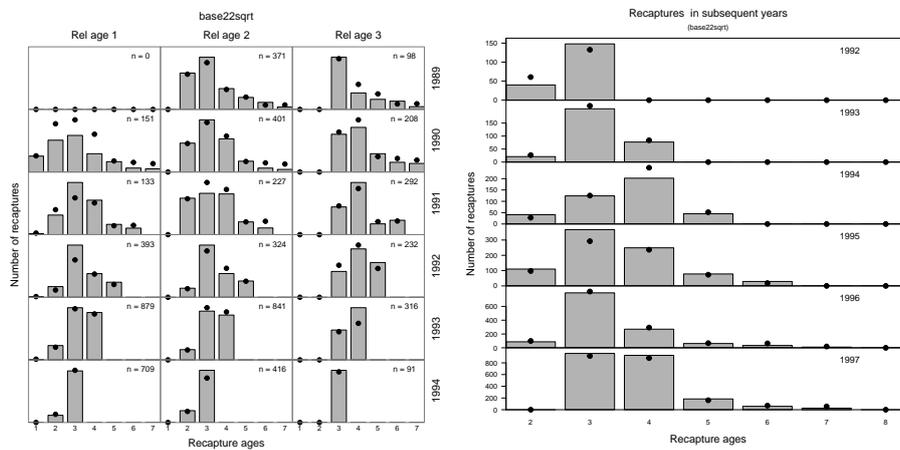

Figure 4.5: *For the best fitting grid conventional mark-recapture data fitting summaries for the tagger-aggregated (left) and pooled-to-recapture-year scenarios.*

presence of anomalous year-effects due to adult sampling processes. Figure 4.6 summarises the predictive distribution of the POPs at these three aggregation levels. For these three POP aggregation levels the predictive p-values were 0.48, 0.59 and 0.85, respectively.

For the HSPs the data are less sparse; there are only two covariates the birth cohort of each juvenile in the comparison. For these data we plot the predictive summaries at the main level and when aggregated to the total number of HSPs for the given earliest cohort in the comparison. Figure 4.7 details these predictive summaries. For the oldest cohort aggregation level the predictive p-value was 0.27.

The predictive summaries for the total number of POPs and HSPs can be found in Figure 4.8.

5 Population dynamic summaries

The primary population dynamic summaries are the relative Total Reproductive Output (TRO) and recruitment - booth are summarised in Figure 5.1. Table 5.1 details the general status
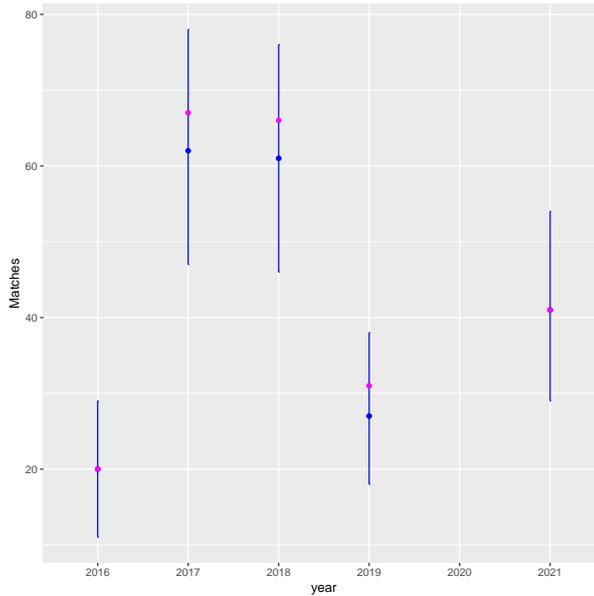
Figure 4.6: *Predictive summary for the gene tagging data. Magenta dots are the observations and blue full and dotted lines are the predictive median and 95% interval, respectively.*

summary statistics used in previous years [3].

Variable	Summary
ΔTRO	0.23 (0.2–0.28)
$\Delta B10p$	0.21 (0.19–0.26)
F/F_{msy}	0.49 (0.34–0.66)
B_{msy}/B_0	0.3 (0.22–0.35)
B_y/B_{msy}	0.83 (0.6–1.26)
MSY	30,648 (29,142–31,426)

Table 5.1: *Stock status summary in terms of median (80% CI).*

6   Discussion

This paper details an exploration of including the most recent assessment data into the CCSBT Operating Model, using the grid from 2020 [3] as the default initial grid configuration. The OM was fitted to each of the unique 216 grids with no obvious convergence issues, and 2,000 samples were successfully drawn (using the previously agreed resampling strategy) to create a reference set of OMs from which to explore how well the model explains the data. The resultant grid (Figure 3.1) showed that for both parameters resampled using the full objective function (M_0 and M_{10}) that the central grid element was sampled the most and was relatively balance for the elements at the upper and low extremes. For this initial exploration at least, this suggests that the current range of these parameters seems appropriate. We do not use objective function resampling for steepness and have not explored this option herein. Previous work [6] showed that the preference for lower values of steepness driven by the recruitment penalty was both decadally highly variable and, when accounting properly for temporal autocorrelation, much weaker than previously thought. It would be prudent to revise the analyses in [6] at the OMMP to establish if
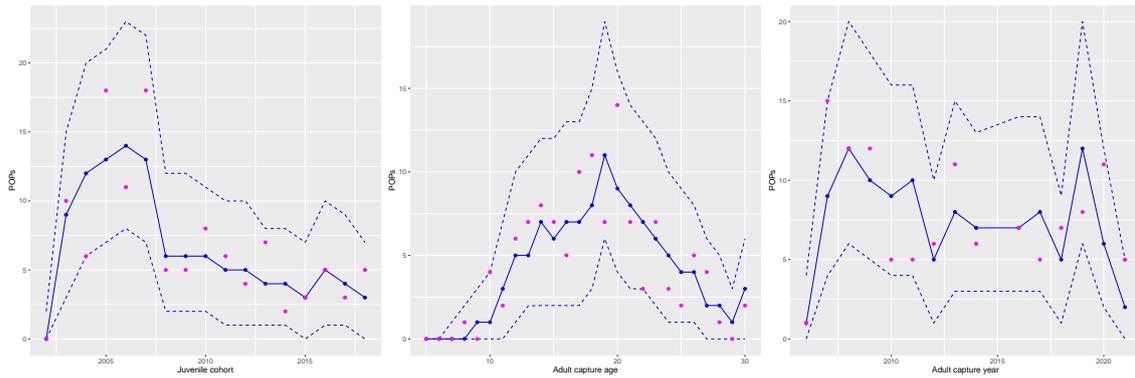
Figure 4.7: *Predictive summary for the POPs at the juvenile cohort (left), adult capture age (middle) and adult capture year (right) aggregation levels. Magenta dots are the observations and blue full and dotted lines are the predictive median and 95% interval, respectively.*

Figure 4.8: *Predictive summary for the HSPs at the base (left) and oldest juvenile cohort (right) aggregation levels. Magenta dots are the observations and blue full and dotted lines are the predictive median and 95% interval, respectively.*
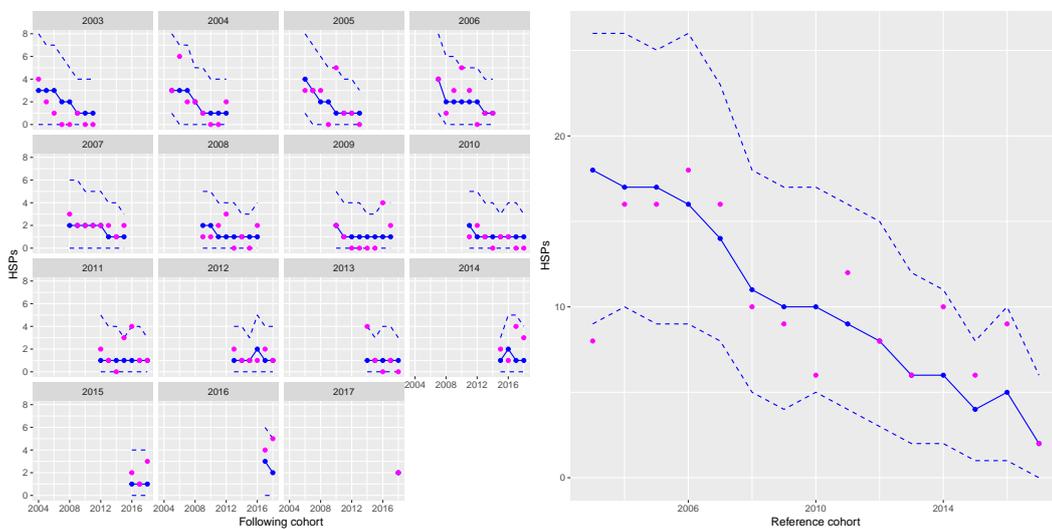
this is still the case as it will be central to discussing an appropriate range for the steepness in the grid.

Fits to the age and size frequency data are good for when levels of sampling are high, with no obviously pathological issues in particular for the major fisheries (LL_1, Indonesian and surface). The fits to the revised single GAM-derived CPUE index are good - though the model struggle a little to fully explain the historically high 2022 point. Fits to the aerial survey index and 1990s tagging data are very much as seen previously. Fits the to gene tagging data are good - recall though that there is no 2020 estimate but there is a 2021 estimate so 5 now in total. The fits to the CKMR data are all good - for the POPs and HSPs at the usual aggregation levels and very good for overall kin pairs.

The estimate range of relative TRO in terms of median (and 80% CI) was 0.23 (0.2–0.28) so a 15% increase from 2020 levels - this is consistent with the 5% annual growth rate in the TRO since around 2012, driven by both the POPs and now the longline CPUE. In terms of recruitment
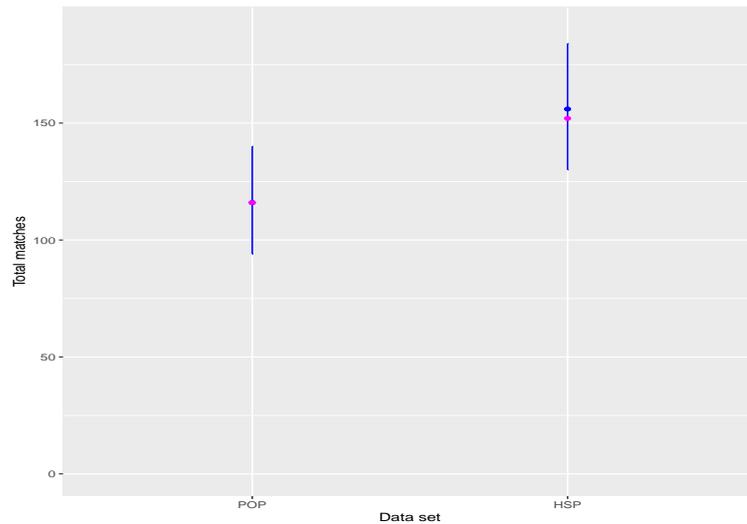
Figure 4.9: *Predictive summary overall number of POPs (left) and HSPs (right). Magenta dots are the observations and blue full and dotted lines are the predictive median and 95% interval, respectively.*

the 2019 year class would be the last one with observed information. For 2018 a very high value is estimated driven by the historically high CPUE point in 2022; for 2019 the gene tagging estimate is very close to the average age 2 abundance and brings down the estimate in this year. Recall again we do not have a gene tagging estimate for 2020 (the 2018 cohort) so the CPUE is really the only index likely to be observing this cohort at this time. Other key status summaries all show continued recovery of the stock with estimated MSY levels very similar to previous years.
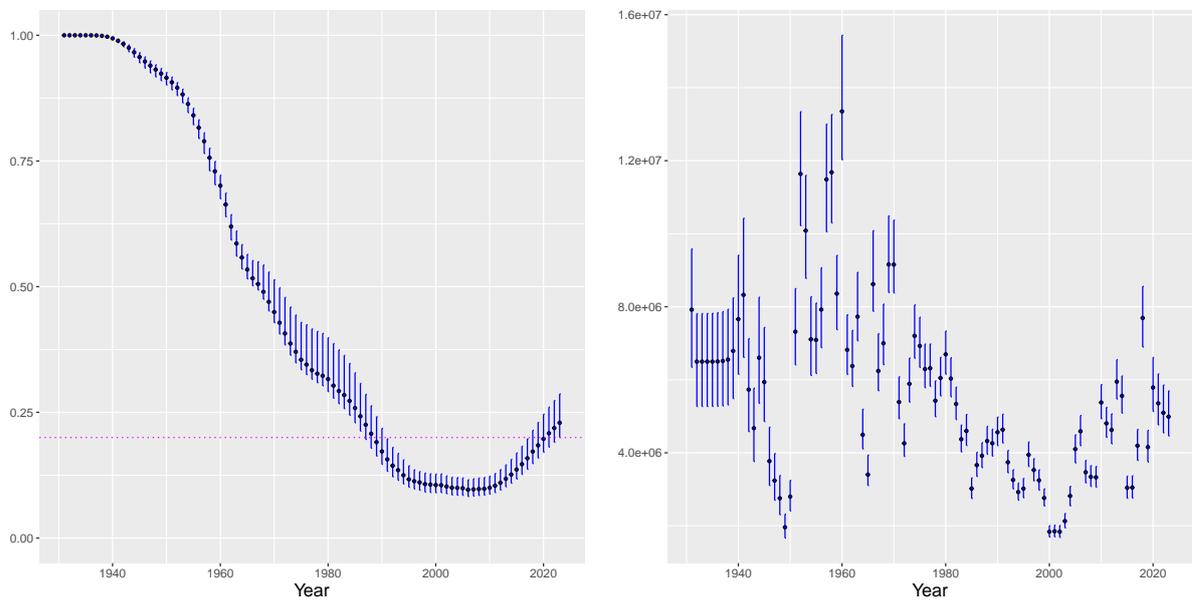
7   Acknowledgements

Figure 5.1: *Relative TRO (left) and recruitment (right) median and approximate 90% CI.*

References

[1] Anon. (2020). Report of the 25th meeting of the Extended Scientific Committee.

[2] Anon. (2022). Report of the 27th meeting of the Extended Scientific Committee.

[3] Hillary, R. *et al.* (2020) The assessment of stock status in 2020. *CCSBT–ESC/2009/12*.

[4] Gelman, A., Carlin, B.J., Stern, H.S., Rubin, R.B. (1995) Bayesian Data Analysis. *Chapman and Hall, London*.

[5] Meng, X. (1994) Posterior predictive p-values. *Annal. Stats.* **22**: 1142–1160.

[6] Hillary, R., Preece, A., and Davies, C. (2020) Information breakdown for steepness parameter in the CCSBT OM. *CCSBT–ESC/2008/13*.

WE DO THE EXTRAORDINARY
EVERY DAY
We innovate for tomorrow and help improve today for our customers, all Australians and the world.
Our innovations contribute billions of dollars to the Australian economy every year. As the largest patent holder in the nation, our vast wealth of intellectual property has led to more than 150 spin-off companies.
With more than 5,000 experts and a burning desire to get things done, we are Australias catalyst for innovation.
WE IMAGINE. WE COLLABORATE.
WE INNOVATE.